Journal of Applied Mathematics and Physics, 2022, 10, 772-778
https://www.scirp.org/journal/jamp
ISSN Online: 2327-4379
ISSN Print: 2327-4352

Tunning the Band Gap of 1T'-WTe_2 by Uniaxial Strain

Jingyi Liu

College of Science, University of Shanghai for Science and Technology, Shanghai, China
Email: 1259571560@qq.com

How to cite this paper: Liu, J.Y. (2022) Tunning the Band Gap of 1T'-WTe_2 by Uniaxial Strain. *Journal of Applied Mathematics and Physics*, **10**, 772-778.
https://doi.org/10.4236/jamp.2022.103053

Received: February 10, 2022
Accepted: March 12, 2022
Published: March 15, 2022

Abstract

The QSH edge channels can be used to connect dissipationless nanoelectronic devices, when the topological edge states and the bulk states have the perfectly spaced. But the monolayer 1T'-WTe_2 bulk state is metallic nature, with edge channel lengths around 100 nm, which hinders its further study. By simulating the different terminational edge states, using the GGA-1/2 method to calculate, we found a stable terminational edge state. And under strain engineering, fixed the a-axis, the band gap gradually increases with the b-axis tensile. When the tensile to 2.9%, the band gap increases to 245 meV. It greatly improves the application of 1T'-WTe_2. During the phase transition of the material from half-metal to insulator, the topology of edge states remains unchanged, showing strong robustness. Thus introducing strain can make 1T'-WTe_2 a suitable material for fundamental research or topological electronic devices.

Keywords

1T'-WTe_2, Band Gap, Uniaxial Strain, GGA-1/2

1. Introduction

Two-dimensional transition metal dichalcogenides have unique properties, it has been widely concerned by the physics community. Two-dimensional transition metal dichalcogenides can exist in a variety of crystalline phases [1] [2]. For example, the MmoS2 due to the different stack at layer to layer, there have three crystal phases, 2H phase, 1T phase and 1T'phase. After a large number of studies, it has been proved that the 2H phase of Mos_2 is the most stable, and exhibits semiconducting properties [3]. But the 1T phase and the 1T' phase are metallic, and the three phases can be transformed into each other under certain circumstances [4] [5] [6]. In recent years, the distorted phase transition metal

dichalcogenides are considered to have interesting topological properties. Due to spin coupling of edge states, this bulk state opens a certain band gap, while the topological edge states have time-reversal symmetry, show a gapless state [7] [8]. This topological property provides a new idea for the reach the transition metal dichalcogenides.

The monolayer of 1T'-WTe_2 has been confirmed as a topological insulator by various nonlocal transport measurements [9]. Due to the metallic nature of the bulk state, the edge channel length is around 100 nm, which hinders its further study, so it is necessary to regulate the band gap of the bulk state [10]. The regulation of the band gap can be achieved by introducing an electric field. In recent years, it has been found that the electric field is mainly used for TMD materials and superconductivity [11] [12]. For some low-dimensional materials, strain may be a more effective method. For example, strain-engineered Dirac states [13] and strain-regulated band gap [14]. However, the band gap of monolayer 1T'-WTe_2 is always underestimated by ordinary methods, so a more accurate method is needed.

In this paper, we apply a new method to calculate and regulate the band gap of monolayer 1T'-WTe_2 zigzag nanoribbons. Since 1T'-WTe_2 has the tendency of complex band scattering and coexists with edge trivial states. By calculating the different edge states terminate of monolayer 1T'-WTe_2 nanoribbons, we found the best edge state, the reconstructed edge state. In this edge state, the topological edge states are effectively separated from the bulk states. When the width of the nanoribbon is 35.05 Å, by applying strain on the b-axis. We found that the band gap gradually increases/decreases with tensile/compress of the b-axis. The strain is from −2.2% to 2.9%, and the band gap is from 93 meV to 245 meV, realizing a large transition of 152 meV. Make the edge states better separated from the bulk states. By our method, the band gap of monolayer 1T'-WTe_2 nanoribbons is correctly calculated, and through the modulation of the band gap, monolayer 1T'-WTe_2 can be used as a promising strain-tunable topological quantum electron material.

2. Method and Computational Details

The geometric optimizations, as well as calculation of the electronic structures for the above mentioned structures are performed by first-principles method based on the density functional theory (DFT) [15] implemented in the QuantumATK software package [16]. The linear combination of atomic orbitals (LCAO) method was used with generalized gradient approximations −1/2(GGA − 1/2) [17]. Due to the strong SOC in Te atoms, SOC was included in all calculations about electronic structures. The density mesh cutoff energy was chosen to be 160 Ry, and the total energy was converged to better than 10^{-5} eV. The periodic direction of nanoribbon was set to be along y-direction, and the vertical direction of 2D material was set to be the z-direction. The k-points sampling is 1 × 8 × 1. Because of the periodicity of the studied nanoribbons, the vacuum

layer between the left and right adjacent plates in the x and z directions is at least 15 Å. The lattice constant of monolayer 1T'-WTe_2 nanoribbon was set to be about 6.31 Å. The overall structure monolayer 1T'-WTe_2 nanoribbon was optimized, and the final force exerted on each atom is less than 0.01 eV/Å.

3. Results and Discussion

The electronic states of the bulk states of the monolayer 1T'-WTe_2 are spin degenerate, due to the existence of time-reversed states. However, the edge states are broken due to the time-reversal state, so the spin degeneracy of the edge states is expected to be improved. Shown in Figure 1, we calculated six edge states and the band structures. The unit cell of the distorted 1T'-WT2 lattice can be divided into a and b substructures, it is shown in Figure 1(a). By comparing six different edges, we found that the single-W-atom architecture with edge a substructure is not stable. But after the structure is optimized, the W(a) edge becomes a new Te(a') edge, and the reconstruction of the edge makes the structure stable.

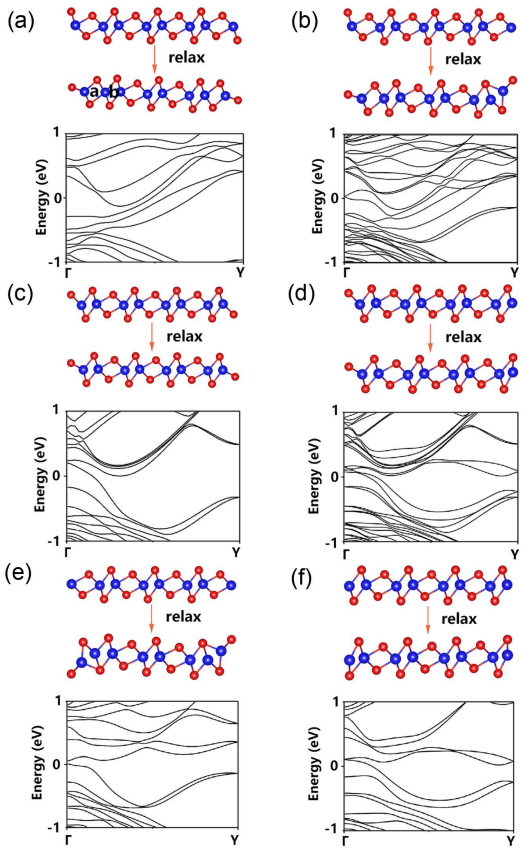

Figure 1. (a) The side view of Te(ab)-(ba)Te nanoribbon, and the structure diagram is below. (b) The side view of Te(ab)-(ba')Te nanoribbon, and the structure diagram is below. (c) The side view of Te(ba)-(ab)Te nanoribbon, and the structure diagram is below. (d) The side view of Te(ba)-(ab)W nanoribbon, and the structure diagram is below. (e) The side view of Te(a'b)-(ba')Te nanoribbon, and the structure diagram is below. (f) The side view of W(ba)-(ab)W nanoribbon, and the structure diagram is below.

From the energy band diagram, we found that the edge states of Te(ab)-(ba)Te, Te(ab)-(ba')Te and Te(ba)-(ab)W are mixed with the bulk states, which are not easy to observe. The Te(ba)-(ab)Te, Te(a'b)-(ba')Te and W(ba)-(ab)W bulk states are separated from the edge states. Although the edge states partially sink into the bulk states, we can clearly observe the edge states. By computing these three different edge states, we found that the Te(a'b)-(ba')Te has the best stability. And in Table 1 we used three different methods to calculate the band gap of the nanoribbon of the 1T'-WTe_2, the edge structure is Te(a'b)-(ba')Te, and the width is 21.26 Å. The GGA-1/2 method to calculate the band is the best, the traditional GGA method is underrated. In Figure 1(e), the Te(a'b)-(ba')Te nanoribbon because the width is small, there is a certain coupling of edge states. In order to reduce the effect of edge coupling, the width of the nanoribbon can be adjusted. As shown in Figure 2, as the width of the nanoribbon increases, the band gap of the bulk state gradually decreases. And as the width increases, the coupling between the edge states gradually weakens, and the edge states exhibit a perfect Dirac shape near the Fermi energy.

The QSH edge channel can be used as an interconnection in non-dissipative nanoelectronic devices, and the premise of using the QSH as a channel is that the topological edge state of the QSH should be perfectly spaced from the bulk state. So our material is chosen to have a width of 35.05 Å, the Te(a'b)-(ba') edge state of IT'-WTe_2 was used as the research object. Through uniaxial strain, the evolution of the bulk band gap of 1T'-WTe_2 was calculated. Fix the lattice constant of the a-axis, by tensioning or compressing the b-axis, in the range of −2.2% - 2.9%. In Figure 3, after gradually compressing the b-axis, the band gap of the bulk state gradually decreases, and when compressed by 2.2%, the band gap of the bulk state decreases to 93 meV. While tensioning the b-axis, the band gap gradually increases, and when the b-axis is stretched by 2.9%, the band gap increases to 245 meV. A larger band gap means that the monolayer 1T'-WTe_2 nanoribbons have more room for application. Therefore strain is a feasible way to tune the band gap of 1T'-WTe_2.

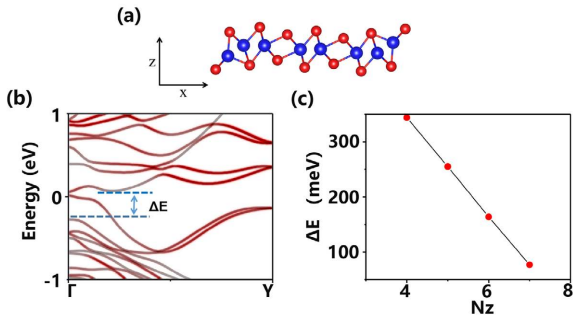

Figure 2. (a) The side view of Te(a'b)-(ba')Te nanoribbon, and the width is 21.26 Å. (b) Band structure of Te(a'b)-(ba')Te nanoribbon. The size of filled red circle is proportional to the LDOS of edges. The bulk state band gap is marked (ΔE). (c) Dependence of the band gap (ΔE) of the Te(a'b)-(ba')Te nanoribbon on the magnitude of the nanorribon width. Nz is the number of W atoms in the nanorribon.

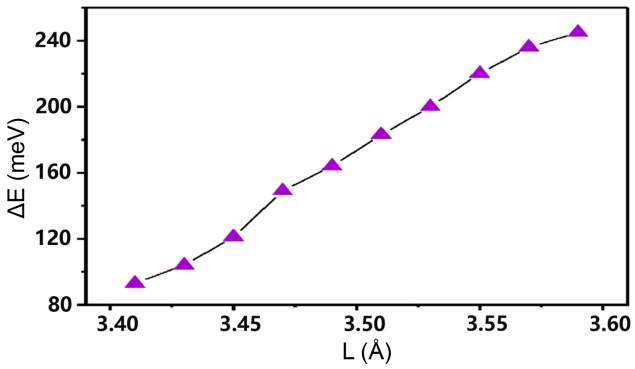

Figure 3. Dependence of the band gap (ΔE) of the Te(a'b)-(ba')Te nanoribbon on the magnitude of the Lattice constant of nanoribbon.

Table 1. The band gap calculated by different methods, when the nanoribbon is 21.26 Å.

Method	GGA	Meta-GGA	GGA-1/2
ΔE (meV)	198	235	344

4. Conclusions

In summer, the PBE method is always underestimated when calculating the band gap, while the GGA-1/2 method has been shown to optimize the band gap calculation. In this paper, GGA-1/2 is used to calculate the energy bands and their stability of 1T'-WTe_2 monolayers with six different terminational edges, and we found most stable structure is Te(a'b)-(ba') edge state. Below this edge state, the band gap of the bulk state can gradually change with the width of the nanoribbon. In order to reduce the influence of the edge coupling effect, we take the nanoribbon width as 35.05 Å. And monolayer of 1T'-WTe_2 nanoribbon with fixed a-axis and tension/compression along the b-axis. Compression along the b-axis, the band gap of the bulk state gradually reduces, while stretching along the b-axis, the band gap of bulk state gradually increases. When tensioning to 2.9%, the bulk band gap increases to 245 meV, enabling 1T'-WTe_2 to successfully change from a semi-metallic phase to an insulating phase. And the edge state has not changed, and still maintains the non-trivial topology. Strain engineering is used to adjust the band gap, which provides an idea for the later study of two-dimensional transition metal dichalcogenides about the topology electronics.

The authors would like to thank the computational resources utilized in this research were provided by Shanghai Supercomputer Center.

Conflicts of Interest

The author declares no conflicts of interest regarding the publication of this paper.

References

[1] Fang, Y.Q. Pan, J., Zhang, D.Q., Wang, D., Hirose, H.T., *et al.* (2019) Discovery of

Superconductivity in 2M WS_2 with Possible Topological Surface States. *Advanced Materials*, **31**, 1901942. https://doi.org/10.1002/adma.201901942

[2] Wang, X.W., Sun, Y.H. and Liu, K. (2019) Chemical and Structural Stability of 2D Layered Materials. 2*D Materials*, **6**, Article No. 042001. https://doi.org/10.1088/2053-1583/ab20d6

[3] Qian, X.F., Liu, J.W., Fu, L. and Li, J. (2014) Quantum Spin Hall Effect in Two-Dimensional Transition Metal Dichalcogenides. *Science*, **346**, 1344-1347. https://doi.org/10.1126/science.1256815

[4] Zhang, C. Kc, S., Nie, Y., Liang, C., Vandenberghe, W.G., Longo, R.C., Zheng, Y., Kong, F., Hong, S., Wallace, R.M. and Cho, K. (2016) Charge Mediated Reversible Metal-Insulator Transition in Monolayer $MoTe_2$ and $WxMo_1$-xTe_2 Alloy. *ACS Nano*, **10**, 7370-7375. https://doi.org/10.1021/acsnano.6b00148

[5] Keum, D.H., Cho, S., Kim, J.H., Choe, D.-H., *et al.* (2015) Bandgap Opening in Few-Layered Monoclinic $MoTe_2$. *Nature Physics*, **11**, 482-486. https://doi.org/10.1038/nphys3314

[6] Lin, Y.-C., Dumcenco, D.O., Huang, Y.-S. and Suenaga, K. (2014) Atomic Mechanism of the Semiconducting-to-Metallic Phase Transition in Single-Layered MoS_2. *Nature Nanotechnology*, **9**, 391-396. https://doi.org/10.1038/nnano.2014.64

[7] Tang, S., Zhang, C., Wong, D., *et al.* (2017) Quantum Spin Hall State in Monolayer 1T'-WTe_2. *Nature Physics*, **13**, 683-687. https://doi.org/10.1038/nphys4174

[8] Xu, S.-Y., Ma, Q., Shen, H., *et al.* (2018) Electrically Switchable Berry Curvature Dipole in the Monolayer Topological Insulator WTe_2. *Nature Physics*, **14**, 900-906. https://doi.org/10.1038/s41567-018-0189-6

[9] Fei, Z., Palomaki, T., Wu, S., Zhao, W., Cai, X., Sun, B., Nguyen, P., Finney, J., Xu, X. and Cobden, D.H. (2017) Edge Conduction in Monolayer WTe_2. *Nature Physics*, **13**, 677-682. https://doi.org/10.1038/nphys4091

[10] Wu, S., Fatemi, V., Gibson, Q.D., Watanabe, K., Taniguchi, T., Cava, R.J. and Pablo, J.-H. (2018) Observation of the Quantum Spin Hall Effect up to 100 Kelvin in a Monolayer Crystal. *Science*, **359**, 76-79. https://doi.org/10.1126/science.aan6003

[11] Wang, Y., Xiao, J., Zhu, H., Li, Y., Alsaid, Y., Fong, K.Y., Zhou, Y., Wang, S., Shi, W., Wang, Y., Zettl, A., Reed, E.J. and Zhang, X. (2017) Structural Phase Transition in Monolayer $MoTe_2$ Driven by Electrostatic Doping. *Narure*, **550**, 487-491. https://doi.org/10.1038/nature24043

[12] Sajadi, E., Palomaki, T., Fei, Z., Zhao, W., Bement, P., Olsen, C., Luescher, S., Xu, X., Folk, J., *et al.* (2018) Gate-Induced Superconductivity in a Monolayer Topological Insulator. *Science*, **362**, 922-925. https://doi.org/10.1126/science.aar4426

[13] Liu, Y., Li, Y.Y., Rajput, S., Gilks, D., Lari, L., Galindo, P.L., Weinert, M., Lazarov, V.K. and Li, L. (2014) Tuning Dirac States by Strain in the Topological Insulator Bi_2Se_3. *Nature Physics*, **10**, 294-299. https://doi.org/10.1038/nphys2898

[14] Zhao, C., Hu, M., Qin, J., Xia, B., Liu, C., *et al.* (2020) Strain Tunable Semimetal-Topological-Insulator Transition in Monolayer 1T'-WTe_2. *Physical Review Letters*, **125**, Article No. 046801. https://doi.org/10.1103/PhysRevLett.125.046801

[15] Brandbyge, M., Mozos, J.-L., Ordejón, P., Taylar, J. and Stokbro, K. (2002) Density-Functional Method for Nonequilibrium Electron Transport. *Physical Review B*, **65**, Article No. 165401. https://doi.org/10.1103/PhysRevB.65.165401

[16] Smidstrup, S. Markussen, T. Vancraeyveld, P., *et al.* (2020) QuantumATK: An Integrated Platform of Electronic and Atomic-Scale Modelling Tools. *Journal of Physics*: *Condensed Matter*, **32**, Article No. 015901.

https://doi.org/10.1088/1361-648X/ab4007

[17] Ferreira, L.G. Marques, M. and Teles, L.K. (2011) Slater Half-Occupation Technique Revisited: The LDA-1/2 and GGA-1/2 Approaches for Atomic Ionization Energies and Band Gaps in Semiconductors. *AIP Advances*, **1**, Article No. 032119. https://doi.org/10.1063/1.3624562